TELKOMNIKA Telecommunication, Computing, Electronics and Control
Vol. 24, No. 6, December 2026, pp. 1915∼1927
ISSN: 1693-6930, DOI: 10.12928/TELKOMNIKA.v24i6.28132

Adaptive OFDM/OTFS switching for high-mobility wireless communications

Nessrine Smaili[1], Dihia Amani[1], Feriel Razaoui[1], Mustapha Djeddou[2]
[1]Institute of Electrical and Electronic Engineering, University M'Hamed Bougara-Boumerdes, Boumerdes, Algeria
[2]Industrial Engineering Department, National Polytechnic School, Algiers, Algeria

Article Info

Article history:

Received Jun 22, 2026
Revised Aug 1, 2026
Accepted Oct 11, 2026

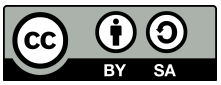
Keywords:

Bit error rate
Doubly selective channel
Orthogonal frequency division multiplexing
Orthogonal time-frequency space
Sixth generation

ABSTRACT

High-mobility wireless communication introduces Doppler shifts that degrade the performance of conventional modulation schemes. Orthogonal frequency division multiplexing (OFDM) remains efficient in low-mobility conditions but suffers significant degradation as user speed increases, whereas orthogonal time-frequency space (OTFS) modulation offers superior robustness in high-mobility, doubly selective channels at the cost of higher implementation complexity. This paper proposes a hybrid OFDM/OTFS system that estimates user's velocity in real time and dynamically switches between the two waveforms to maintain reliable performance across mobility conditions. Simulations show OTFS performs better at high speeds, while OFDM is more efficient at low speeds, confirming the benefit of adaptive switching over either waveform alone. Beyond bit-error-rate gains, the proposed framework illustrates how waveform flexibility can support the diverse mobility requirements of future sixth generation (6G) networks.

This is an open access article under the CC BY-SA license.



Corresponding Author:

Nessrine Smaili
Institute of Electrical and Electronic Engineering, University M'Hamed Bougara-Boumerdes
Boumerdes, Algeria
Email: n.smaili@univ-boumerdes.dz

1. INTRODUCTION

The development of wireless communication systems has been driven by the desire for higher data rates, lower latency, and better reliability, especially in mobile environments such as vehicular networks [1]. As the transition from fifth generation (5G) networks to sixth generation (6G) networks is made, doubly selective channels combining rapid time variation with frequency selectivity arising from multipath propagation and Doppler effects pose major challenges for conventional modulation schemes [2], motivating researchers to develop innovative and useful communication techniques [3], [4].

Orthogonal frequency division multiplexing (OFDM) has been a cornerstone of fourth generation (4G) and 5G technologies due to its simplicity and efficiency in handling frequency-selective channels [5]. However, OFDM performance significantly deteriorates under high Doppler shifts, as it assumes quasi-static channel conditions over each symbol duration [6], and it suffers from sensitivity to Doppler spread and inter-carrier interference (ICI) in high-mobility environments [7]. Various enhancements have been proposed, including adaptive cyclic prefixing (CP) and Doppler-resilient equalization, but these methods only partially address the core limitations in rapidly varying channels, motivating investigation of alternative waveforms [2].

Orthogonal time frequency space (OTFS) modulation has recently emerged as a promising approach

to wireless communication with high mobility [2]. Unlike OFDM, which operates in the time-frequency domain, OTFS maps information symbols to the Delay-Doppler domain, giving it greater robustness to Doppler effects and favorable performance in mobile environments [6], [8]. For example, Hadani *et al.* [9] introduced the theoretical foundation for OTFS modulation, demonstrating its superior bit error rate (BER) performance under Doppler effects, and subsequent work [10], [11] expanded this with detection algorithms (e.g., message passing algorithm (MPA) and linear minimum mean square error (LMMSE)) and receiver designs tailored to the Delay-Doppler domain. However, in low-mobility environments where Doppler effects are limited, the performance advantage of OTFS becomes less significant, while its higher computational complexity may reduce implementation efficiency compared with OFDM [12]. To overcome this issue, the objective of this work is to achieve reliable and efficient communication regardless of the speed of the user, by adapting the modulation technique to mobility scenarios.

Hybrid modulation approaches combining OFDM and OTFS have also been explored. Study [13] explored switching based on signal-to-noise ratio (SNR) thresholds, while author [14] suggested using channel coherence time to trigger modulation changes; both, however, relied on fixed thresholds and did not dynamically adapt to changing user mobility in real time. Closer to the present work, Darghouthi *et al.* [15] also proposed a mobile-speed-based OFDM/OTFS switching strategy, aided by an integrated sensing and communication (ISAC) radar for Doppler estimation. The present work differs in its estimator design combining LMMSE channel estimation with a phase-based Doppler estimator for OFDM and a Delay-Doppler energy-peak estimator for OTFS, rather than relying on an external radar sensing subsystem and in deriving its switching threshold directly from the BER crossover behavior observed between the two waveforms section 3.3, giving a direct, self-contained mapping between physical user motion and modulation choice.

2. PROPOSED METHOD

2.1. OFDM system model

OFDM is a widely adopted multicarrier modulation technique that efficiently transmits high-rate data over wireless channels. By dividing the available bandwidth into multiple orthogonal subcarriers, OFDM enables parallel data transmission, which enhances spectral efficiency and robustness against frequency-selective fading. Its inherent resistance to multipath interference and ease of equalization have made it the foundation of many modern wireless standards, including long-term evolution (LTE) and wireless fidelity (Wi-Fi). In OFDM, each subcarrier is modulated independently, allowing the system to efficiently handle severe channel conditions such as multipath propagation and narrowband interference. The orthogonality of the subcarriers ensures that they do not interfere with each other even though their spectra overlap, which maximizes spectral utilization. Additionally, the use of a CP helps to mitigate inter-symbol interference (ISI) caused by delayed signal paths in the channel.

A typical OFDM system consists of a transmitter and a receiver, each performing a series of signal processing operations to map input data onto subcarriers, transmit the signal over the wireless channel, and recover the original information at the receiver. Figure 1 illustrates the fundamental structure of an OFDM transceiver, highlighting the main functional blocks at both the transmitter and receiver sides.

At the transmitter, digital modulation (quadrature amplitude modulation (QAM) and phase shift keying (PSK)) is first performed on the bitstream to create the digital symbols. The digital symbols are fed into a serial-to-parallel (S/P) converter that splits the serial bitstream into N parallel bitstreams, each stream feeding a different subcarrier. Afterward, pilot symbols are inserted among the data symbols to help with channel estimation at the receiver. Next, an inverse fast Fourier transform (IFFT) is performed on the frequency-domain data to convert them to time-domain data so that multiple symbols can be transmitted simultaneously without interference. The time-domain OFDM signal, obtained using the IFFT, is given by (1).

$$x_n = \frac{1}{N} \sum_{k=0}^{N-1} X_k \, e^{j \frac{2\pi kn}{N}}, \quad n = 0, 1, \ldots, N-1 \tag{1}$$

where X_k symbolizes the information carried on the k^{th} subcarrier, N is the total number of subcarriers, x_n stands for the time-domain sample of an OFDM transmission, and $e^{j2\pi kn/N}$ represents the orthogonal basis functions of the IFFT.

The CP is added to each OFDM symbol to mitigate ISI and preserve the orthogonality of subcarriers, thereby helping to maintain system performance under multipath fading. The digital signal is then converted

into an analog signal through the digital-to-analog (D/A) converter, sent out to the wireless channel, and is typically degraded by the channel noise and distortion.

At the receiver, the received analog signal is first converted back to digital form using the A/D converter. After that, the CP is removed. Next, the signal goes through an S/P converter to split the data into parallel streams, and a fast Fourier transform (FFT) is then performed to take the signal back to the frequency domain, as:

$$Y_k = \sum_{n=0}^{N-1} y_n \, e^{-j\frac{2\pi kn}{N}}, \quad k = 0, 1, \ldots, N-1 \tag{2}$$

where y_n is the sample in the received time domain (after CP removal) and Y_k is the received symbol corresponding to the k^{th} subcarrier [16]. After the FFT, pilot symbols are extracted for channel estimation and equalization to correct channel distortion; the pilot symbols are then removed so that only data symbols remain, and the parallel-to-serial (P/S) converter recombines the parallel streams into one stream for the demodulator to recover the original data bits.

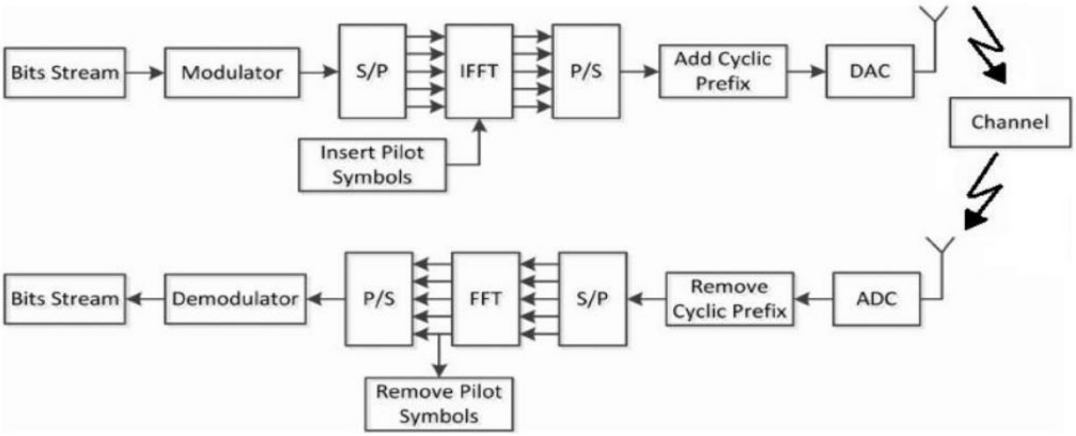


Figure 1. Block diagram of the OFDM transceiver

2.2. OTFS system model

OTFS is an advanced two-dimensional modulation scheme designed to provide robust communication over highly dynamic wireless channels. Unlike traditional OFDM, which operates in the time-frequency domain, OTFS maps information symbols onto the Delay-Doppler domain, effectively transforming a rapidly time-varying channel into a quasi-static one. This unique approach allows each transmitted symbol to experience a nearly constant channel gain, significantly improving performance in high-mobility and Doppler-rich environments. The OTFS transmitter converts Delay-Doppler domain symbols into time-frequency signals using a two-dimensional symplectic Fourier transform, followed by multicarrier modulation similar to OFDM; inverse operations are performed at the receiver to recover the transmitted data from the Delay-Doppler domain. Figure 2 illustrates the block diagram of a typical OTFS transceiver.

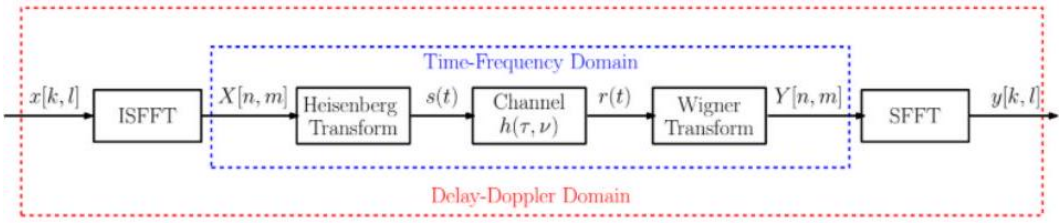


Figure 2. Block diagram of the OTFS transceiver

Mathematically, an OTFS modulator first maps the information symbols $x[k,l]$ in the Delay-Doppler domain to MN symbols $X[n,m]$ in the time-frequency domain using the inverse discrete symplectic finite

Fourier transform (ISFFT), as in (3):

$$X[n,m] = \frac{1}{\sqrt{NM}} \sum_{l=0}^{N-1} \sum_{k=0}^{M-1} x[k,l]\, e^{j2\pi\left(\frac{nk}{N} - \frac{ml}{M}\right)} \tag{3}$$

where M is equivalent to the number of subcarriers in an OFDM symbol, N is equivalent to the number of OFDM symbols contained in one frame, $k = 0, 1, \ldots, M-1$ is the delay axis index, and $l = 0, 1, \ldots, N-1$ is the Doppler axis index. The inner summation is the inverse discrete Fourier transform (IDFT) of X_{dd} along the Doppler dimension, and the outer summation is the DFT along the delay dimension. The ISFFT reduces to (4):

$$X[n,m] = \frac{1}{M} \mathrm{FFT}\Big(\mathrm{IFFT}\big(x_{dd}^{T}\big)^{T}\Big) \tag{4}$$

Once the symbols are in the time-frequency domain, they are mapped to a continuous-time transmit signal $s(t)$, also known as the waveform. This process involves pulse shaping with a transmit pulse $g_{tx}(t)$ to support matched filtering at the receiver and eliminate cross-symbol interference at the OTFS demodulator; $s(t)$ is obtained by performing the Heisenberg transform:

$$s(t) = \sum_{n=0}^{N-1} \sum_{m=0}^{M-1} X[n,m]\, g_{tx}(t - nT)\, e^{j2\pi m\Delta f(t-nT)} \tag{5}$$

This generalizes the OFDM inverse Fourier transform but operates on a 2D time-frequency grid, enabling Delay-Doppler domain signal localization. At the receiver, the received signal $r(t)$ of an OTFS system may be expressed as (6):

$$r(t) = \int_{-\infty}^{\infty} H(t,f) S(f)\, e^{j2\pi ft}\, df \tag{6}$$

where $H(t,f)$ is the time-frequency channel and $S(f) = \mathcal{F}(s(t))$ is the frequency spectrum of the continuous-time transmit signal $s(t)$. As the Heisenberg transform converts a symbol $X[n,m]$ into a signal $s(t)$, the Wigner transform converts a signal $r(t)$ into a symbol $Y[n,m]$, implemented by applying a matched filter with respect to the transmit pulse g_{tx} and computing the cross-ambiguity function, as in (7):

$$Y(t,f) = \int_{-\infty}^{\infty} g_{rx}^{*}(t-\tau)\, r(t)\, e^{-j2\pi f(t-\tau)}\, dt \tag{7}$$

The cross-ambiguity function $Y(t,f)$ is time-sampled as $\tau = nT$ and frequency-sampled as $f = m\Delta f$ to yield $Y[n,m]$, as in (8):

$$Y[n,m] = Y(t,f)\big|_{\tau=nT,\, f=m\Delta f} \tag{8}$$

After the Wigner transform, the obtained symbols $Y[n,m]$ are transformed into the Delay-Doppler domain using the SFFT [17]:

$$y[k,l] = \frac{1}{\sqrt{NM}} \sum_{n=0}^{N-1} \sum_{m=0}^{M-1} Y[n,m]\, e^{-j2\pi\left(\frac{nk}{N} - \frac{ml}{M}\right)} \tag{9}$$

To recover the transmitted symbols, it is necessary to understand how the signal propagates through the doubly selective wireless channel, which introduces both delay and Doppler effects. The complex baseband received signal after passing through such a channel can be expressed as in (10):

$$r(t) = \iint h(\tau,\nu)\, s(t-\tau)\, e^{j2\pi\nu(t-\tau)}\, d\tau\, d\nu + w(t) \tag{10}$$

where $h(\tau,\nu)$ is the channel spreading function, $s(t-\tau)$ is the transmitted signal delayed by τ, and $e^{j2\pi\nu(t-\tau)}$ introduces a frequency shift due to Doppler effects; $w(t)$ is additive white Gaussian noise (AWGN). Time

dispersion, due to multipath delays, causes frequency-selective fading, while frequency dispersion, due to Doppler shifts caused by motion, leads to time-selective fading. The channel response $h(\tau, \nu)$ is given by (11):

$$h(\tau, \nu) = \sum_{i=1}^{P} h_i \, \delta(\tau - \tau_i) \, \delta(\nu - \nu_i) \tag{11}$$

where P is the number of paths, δ is the Dirac delta function, and h_i, τ_i, and ν_i represent the path gain, delay, and Doppler shift corresponding to the i^{th} path, respectively [18]. Channel estimation methods are used to determine how the channel distorts the transmitted signal, after which equalization methods reverse these distortions and restore the original signal.

2.3. Proposed hybrid system

Recent studies have confirmed the superiority of OTFS over OFDM in high-mobility and doubly selective channels. Compagnoni *et al*. [19] demonstrated significant performance gains of OTFS in high-speed vehicular communication scenarios. Similarly, Khadum *et al*. [20] reported improved BER performance for OTFS over OFDM across extended vehicular A model (EVA), extended typical urban model (ETU), unmanned aerial vehicle (UAV), and doubly selective channel models. Furthermore, Filho *et al*. [21] showed that OTFS consistently outperforms OFDM under severe Doppler and multipath propagation conditions, and this trend is echoed across recent 6G waveform surveys [22]-[24]. While these studies provide valuable comparative analyses, they generally assume the use of a single waveform regardless of mobility conditions. In practice, OFDM remains attractive in static and low-mobility environments due to its lower implementation complexity, whereas OTFS becomes advantageous as user mobility increases.

Motivated by these observations, this work proposes an adaptive velocity-aware hybrid OFDM/OTFS framework that dynamically estimates user velocity and selects the most suitable waveform according to the channel conditions. By combining the efficiency of OFDM in low-mobility scenarios with the robustness of OTFS in highly dynamic environments, the proposed scheme aims to ensure reliable communication performance across a broad range of mobility conditions while supporting waveform flexibility for future wireless networks. The main innovation is the implementation of velocity-based switching logic, allowing seamless transitions between OFDM and OTFS to maintain optimal BER performance across a wide range of speeds.

As illustrated in Figure 3, the proposed model operates by first estimating the speed of the user and comparing it with a predefined velocity threshold (V_{th}). If the speed is below V_{th}, OFDM is selected; otherwise, OTFS is used. During data transmission, the system continuously monitors the user speed in each frame. If the current mode remains suitable for the detected mobility condition, it remains active; otherwise, the system switches to the other mode.

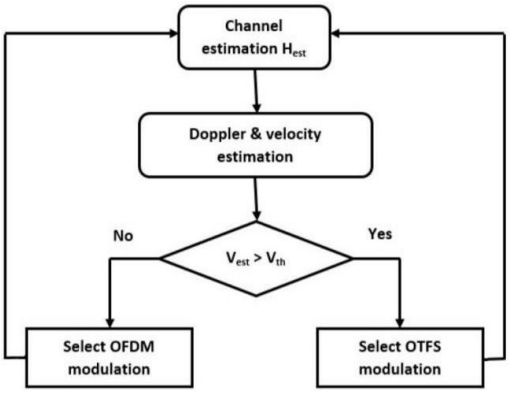


Figure 3. OFDM-OTFS hybrid switching flowchart

2.4. Estimation techniques for the proposed hybrid system

In the proposed hybrid OFDM/OTFS system, the selection of the appropriate waveform depends on accurate estimation of the channel state and Doppler frequency. Pilot-assisted channel estimation is first performed, followed by Doppler estimation and velocity calculation.

2.4.1. LMMSE channel estimation

Known pilot symbols are inserted into the transmitted frame. Let X_p denote the transmitted pilot symbol and Y_p the corresponding received pilot. The received pilot is modeled as in (12):

$$Y_p = H_p X_p + W_p \tag{12}$$

where H_p represents the channel coefficient at the pilot position and W_p is AWGN. The least squares (LS) estimate of the channel is first obtained as in (13):

$$\widehat{H}_{LS} = \frac{Y_p}{X_p} \tag{13}$$

To improve estimation accuracy, the LMMSE estimator is applied as in (14):

$$\widehat{H}_{LMMSE} = R_{HH} \left(R_{HH} + \sigma_n^2 I \right)^{-1} \widehat{H}_{LS} \tag{14}$$

where R_{HH} is the channel autocorrelation matrix, σ_n^2 denotes the noise variance, and I is the identity matrix. The estimated channel is then interpolated over all OFDM subcarriers or across the complete OTFS Delay-Doppler grid.

2.4.2. Doppler estimation in OFDM

In OFDM systems, Doppler shifts produce phase rotation between consecutive pilot symbols. The phase difference between two received pilot symbols is calculated as:

$$\Delta\phi = \angle \left(Y_p(n+1)\, Y_p^*(n) \right) \tag{15}$$

where $(\cdot)^*$ denotes complex conjugation. The Doppler frequency estimate is then obtained by (16):

$$f_d = \frac{\Delta\phi}{2\pi T_s} \tag{16}$$

where T_s is the OFDM symbol duration. After channel estimation, equalization is performed using a one-tap frequency-domain equalizer:

$$\widehat{X}(k) = \frac{Y(k)}{\widehat{H}(k)} \tag{17}$$

where $Y(k)$ is the received symbol on the k^{th} subcarrier and $\widehat{H}(k)$ is the estimated channel response.

2.4.3. Doppler estimation in OTFS

In OTFS modulation, the received symbols are represented in the Delay-Doppler domain. The received OTFS frame can be expressed as in (18):

$$Y[k,l] = H[k,l]\, X[k,l] + W[k,l] \tag{18}$$

where $H[k,l]$ is the channel response in the Delay-Doppler domain. The dominant Doppler tap is determined from the maximum channel energy location as in (19):

$$(\widehat{k}, \widehat{l}) = \arg\max_{k,l} |H[k,l]|^2 \tag{19}$$

The estimated Doppler frequency is then obtained from the Doppler index $\widehat{l}$ as $f_d = \widehat{l}/(NT)$, where N is the number of Doppler bins and T is the frame duration.

2.4.4. Maximal ratio combining (MRC) detection in OTFS

After Doppler estimation, OTFS symbols are detected using MRC [25]. The combined signal is computed as:

$$g_m = \sum_{l \in \mathcal{L}} K_{m+l,l}^H \, b_m^l \tag{20}$$

where $K_{m+l,l}^H$ denotes the Hermitian transpose of the channel coefficient matrix and b_m^l is the interference-cancelled received signal. The normalization factor is given by:

$$D_m = \sum_{l \in \mathcal{L}} K_{m+l,l}^H K_{m+l,l} \tag{21}$$

The estimated transmitted symbol is therefore given by $\widehat{x}_m = D_m^{-1} g_m$. Finally, symbol decisions are obtained using the nearest constellation point detector, as in (22):

$$\widetilde{x}_m = \mathcal{D}\left(\widehat{x}_m\right) \tag{22}$$

2.4.5. Velocity estimation and hybrid switching

The user velocity is estimated from the Doppler frequency according to $v = f_d c / f_c$, where c is the speed of light and f_c is the carrier frequency. The hybrid switching mechanism is defined as in (23):

$$\text{Mode} = \begin{cases} \text{OFDM}, & v < V_{th} \\ \text{OTFS}, & v \geq V_{th} \end{cases} \tag{23}$$

where V_{th} denotes the predefined velocity threshold. The velocity threshold $V_{th} = 120$ km/h was selected based on the crossover behavior observed in the comparative BER analysis (section 3.3): OFDM and OTFS perform comparably between 80 and 180 km/h, after which OTFS's advantage becomes pronounced while OFDM's BER saturates. Placing the threshold within this transition region limits unnecessary mode switching while ensuring the system moves to OTFS before OFDM's performance degrades sharply. The current threshold is fixed and was tuned for the carrier frequency, subcarrier spacing, and channel models used in this study; an adaptive, channel-aware threshold is identified as a direction for future work in section 4.

3. RESULTS AND DISCUSSION

The performance of OFDM and OTFS waveforms has been evaluated using MATLAB simulation on a doubly selective channel. System parameters such as modulation techniques, user velocity, and channel delay profiles were modified to study their impact on system performance.

3.1. Simulation of OFDM performance

Table 1 presents the main parameters used in the OFDM system simulations. Effect of speed: Figure 4 illustrates the BER versus SNR for OFDM using 4-QAM at speeds from 30 to 500 km/h. Increasing SNR reduces BER across all speeds, but higher velocities cause performance degradation due to Doppler-induced ICI and channel variability. CP length effect: Figure 5 illustrates BER performance with varying CP lengths (8, 16, 24 samples) at 30 km/h using 4-QAM. Longer CPs reduce ISI and preserve subcarrier orthogonality in multipath and Doppler conditions, thus lowering BER; however, longer CPs add overhead and delay, reducing spectral efficiency and increasing power consumption. Hence, CP length must balance performance improvements with system efficiency. OFDM with different delay profiles: Figure 6 shows the BER performance of OFDM under EPA, EVA, and ETU delay profiles at 30 km/h. The results indicate that OFDM achieves the best BER performance under the ETU channel, followed by EVA, while EPA presents the highest BER values. This behavior can be explained by the richer multipath diversity provided by channels with larger delay spreads: in the ETU profile, the increased number of delayed propagation paths offers additional frequency diversity, which improves signal detection and reduces BER when appropriate equalization is applied, whereas the EPA profile has a smaller delay spread and therefore provides lower diversity gain, resulting in comparatively weaker performance.

Table 1. OFDM system parameters

Parameters	Values
Data source	Random
Number of subcarriers	64
Number of OFDM symbols	64
Number of frames	1000
Modulation types	QPSK / 4 QAM / 16 QAM / 64 QAM
Carrier frequency (Hz)	4 GHz
Subcarrier spacing (Hz)	15 kHz
Maximum speed (km/h)	30/80/180/500
SNR range (dB)	0 to 20
Cyclic prefix length	16
Channel models	EVA / AWGN

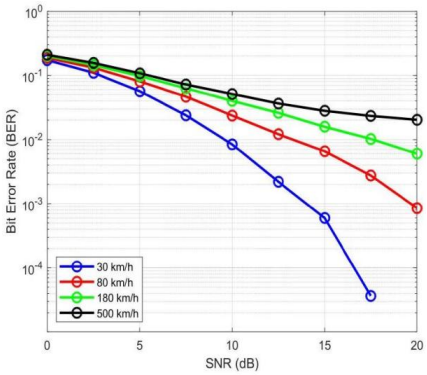


Figure 4. Speed effect on OFDM performance

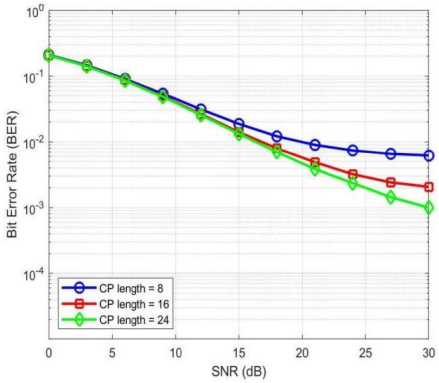


Figure 5. BER vs. SNR CP effect analysis

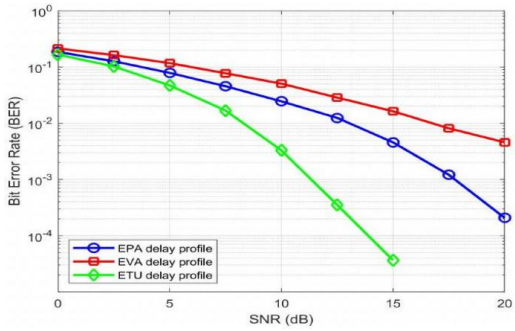


Figure 6. BER vs. SNR with different delay profiles

3.2. Simulation of OTFS performance

Table 2 summarizes the key OTFS simulation parameters used in this study. As shown, the OTFS simulations use 64 delay and Doppler bins under the EVA channel model, adopted as a 3rd generation partnership project (3GPP)-standardized representative multipath profile for vehicular high-mobility scenarios, with a zero-padding length of 4 samples, matching the OFDM configuration in Table 1 to ensure a fair comparison. Understanding the wireless channel in the Delay-Doppler domain is crucial for OTFS modulation, as it uniquely captures how signals spread across multipath delays and Doppler shifts caused by mobility. Figure 7 visualizes the Delay-Doppler power profile of the EVA channel model, highlighting the dominant multipath components that carry the majority of the signal energy.

In OTFS receivers, equalization is a critical step to recover transmitted signals distorted by multipath delays and Doppler shifts, requiring advanced detection algorithms for efficient data decoding. Figure 8 compares the BER performance of three OTFS detectors MPA, block-wise time-domain LMMSE, and MRC at 500 km/h across varying SNR levels. While all detectors perform similarly at low SNR, the MPA detector

consistently achieves the lowest BER due to its iterative processing that effectively mitigates interference and noise. At low SNR, the performance difference between MRC and LMMSE remains limited due to dominant noise effects; the LMMSE detector offers stable equalization considering both channel and noise statistics, while at higher SNR the MRC detector achieves lower BER through efficient signal combining.

Figure 9 presents the BER performance of OTFS at speeds of 30, 180, and 500 km/h across different SNR levels. Interestingly, at high SNR, OTFS achieves better performance at higher speeds (180 and 500 km/h) than at low speed (30 km/h); this is attributed to the increase in Doppler diversity at higher velocities, which OTFS effectively exploits in the Delay-Doppler domain to improve signal detection. These results highlight OTFS's robustness and adaptability across a wide range of mobility scenarios.

Table 2. Key OTFS simulation parameters

Parameters	Values
Data source	Random
Number of Doppler bins (N)	64
Number of delay bins (M)	64
Number of frames	1000
Modulation types	4/16/64 QAM
Carrier frequency (Hz)	4 GHz
Subcarrier spacing (Hz)	15 kHz
Maximum user speed (km/h)	30/180/500
SNR range (dB)	0 to 20
Zero padding length	$M/16 = 4$ samples
Channel model	EVA

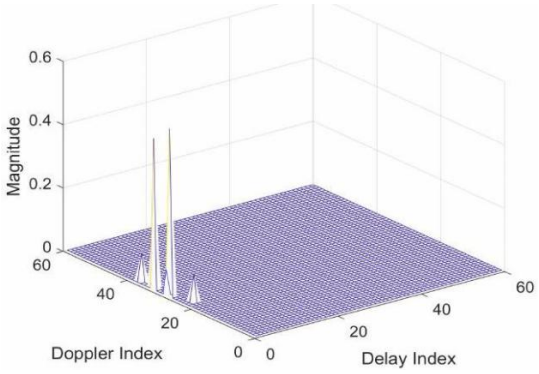


Figure 7. Delay-Doppler representation of EVA multipath channel

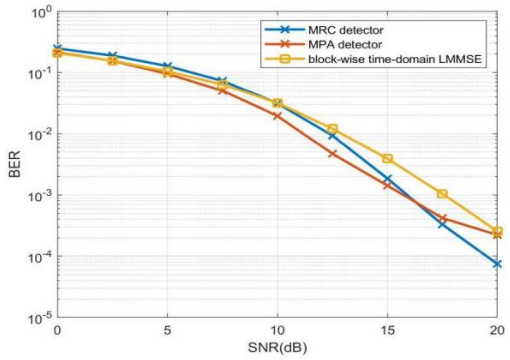


Figure 8. BER vs. SNR for different OTFS detectors

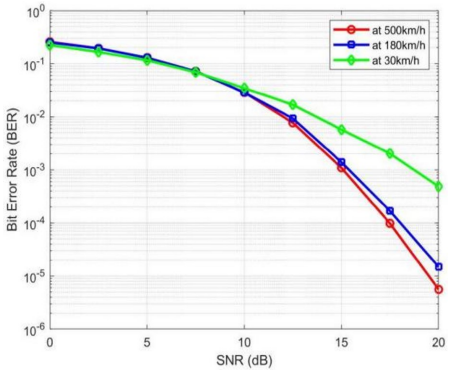


Figure 9. BER vs. SNR OTFS speed effect analysis

3.3. Comparative analysis of OFDM and OTFS at varying mobility speeds

The BER performance comparison of OFDM and OTFS across different mobility speeds is illustrated in Figure 10, which displays results at 30, 80, 180, and 500 km/h. At low speed (30 km/h), OFDM outperforms OTFS due to its effective mitigation of ISI via CP and well-established channel estimation techniques suited for moderate Doppler effects. At moderate speed (80 km/h), both schemes perform comparably at low SNR, but OTFS significantly outperforms OFDM at high SNR by effectively handling increased Doppler spread through Delay-Doppler domain processing. As speed increases to 180 km/h, OFDM's BER saturates due to severe Doppler-induced interference, while OTFS maintains low error rates due to its ability to convert the rapidly varying channel into a nearly time-invariant Delay-Doppler representation. At very high speed (500 km/h), OFDM performance drastically degrades, becoming practically unusable, whereas OTFS maintains robust communication with low BER, leveraging its inherent design to effectively tackle doubly dispersive channels. These results demonstrate the clear advantage of OTFS in high-mobility scenarios, while OFDM remains preferable in low-mobility and moderate channel conditions.

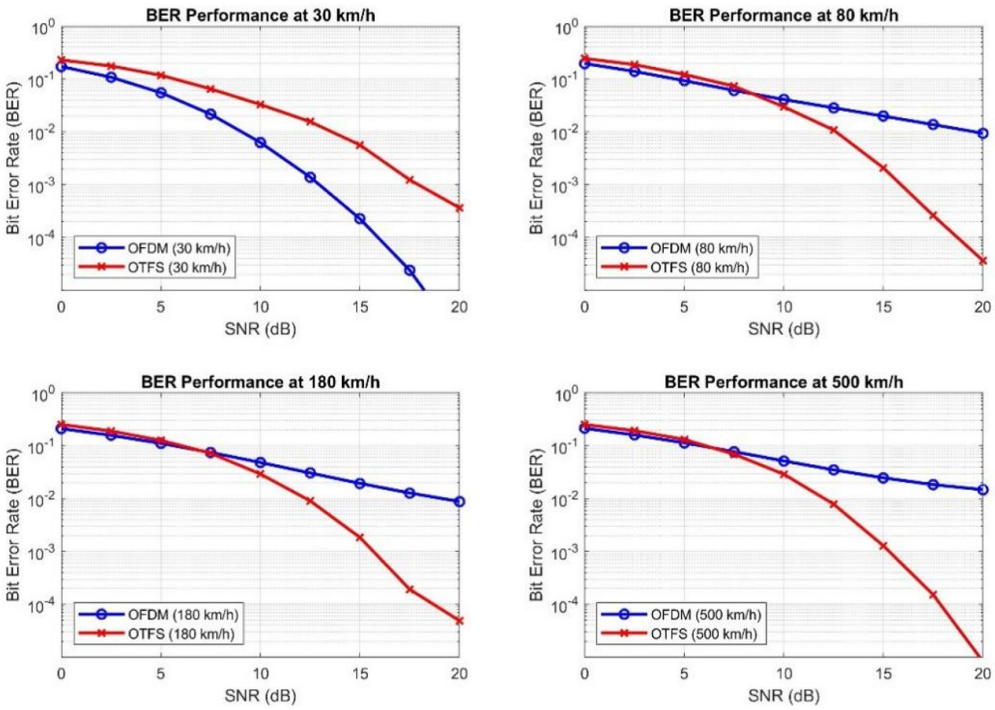


Figure 10. OFDM vs. OTFS BER performance at different speeds

3.4. Hybrid OFDM/OTFS mode switching based on velocity estimation

A hybrid OFDM/OTFS system was implemented with dynamic switching controlled by real-time user speed estimation. After each data packet, the system estimates mobility using pilot-based Doppler techniques and selects the appropriate waveform: OFDM for low speeds and OTFS for high speeds. Table 3 summarizes the key parameters used in this scenario. To evaluate the effectiveness of the hybrid OFDM/OTFS system, its BER was analyzed under different SNR values, with each data packet experiencing a different mobility scenario to assess the system's adaptability to dynamic channel conditions. BER was measured for each packet and plotted versus SNR, as illustrated in Figure 11.

As observed, all packets exhibit similar BER performance across the SNR range, regardless of the modulation scheme used, indicating that the dynamic switching mechanism effectively adapts to mobility variations, ensuring reliable communication and near-optimal error performance. These findings validate the efficiency of the proposed speed-sensitive switching technique: the hybrid system successfully selects the appropriate modulation scheme per packet, providing robust and consistent transmission to users under varying mobility conditions.

It should be noted that the BER results above assume error-free velocity estimation and are based

on a single run of 1000 frames per condition; the sensitivity of the switching decision to Doppler/velocity estimation error under low-SNR conditions, and the statistical variability of the BER curves across repeated independent trials, were not characterized in this study and are identified as necessary additions in section 4. Likewise, while OFDM's per-subcarrier equalization is computationally lighter than OTFS's two-dimensional Delay-Doppler processing and iterative MPA/LMMSE/MRC detection, a quantitative runtime or complexity comparison between the two waveforms was not performed here.

Table 3. Simulation parameters for the hybrid OFDM/OTFS system

Parameter	Value
Speed threshold (V_{th})	120 km/h
SNR	0 to 20 dB
Number of packets	4
Bits per packet	200,000
Speed scenario	80, 180, 30, 500 km/h

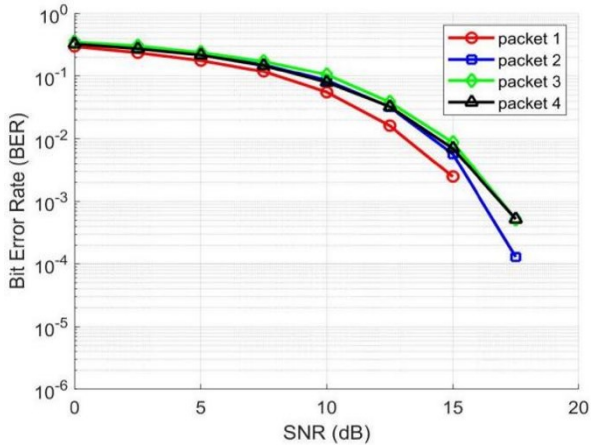


Figure 11. BER vs. SNR for each packet in the hybrid system

4. CONCLUSION

This paper presented a hybrid OFDM/OTFS framework that dynamically adapts modulation to user mobility through real-time velocity estimation. By combining OFDM's efficiency at low speeds with OTFS's robustness under high Doppler conditions, the proposed system maintains reliable performance across the full range of mobility scenarios relevant to 5G and 6G networks. The present evaluation relies solely on simulations under standard channel models (EPA/EVA/ETU, and AWGN) with a fixed velocity threshold; switching delay, hardware implementation cost, and estimation accuracy under low-SNR conditions have not been characterized, and hardware validation under real-world channel conditions remains necessary before the approach can be considered deployment-ready. Future work will focus on integrating the framework with real-time velocity estimation algorithms suited to embedded platforms, adopting an adaptive rather than fixed threshold, testing in live vehicular network trials and extending the switching mechanism to multi-user and massive-multiple-input multiple-output (MIMO) scenarios where mobility profiles differ across users sharing the same channel resources.

FUNDING INFORMATION

Authors state no funding involved.

AUTHOR CONTRIBUTIONS STATEMENT

This journal uses the Contributor Roles Taxonomy (CRediT) to recognize individual author contributions, reduce authorship disputes, and facilitate collaboration.

Name of Author	C	M	So	Va	Fo	I	R	D	O	E	Vi	Su	P	Fu
Nessrine Smaili	✓	✓	✓	✓	✓	✓	✓	✓	✓	✓	✓	✓		
Dihia Amani		✓	✓	✓		✓	✓	✓	✓		✓			
Feriel Razaoui		✓	✓	✓		✓	✓	✓	✓		✓			
Mustapha Djeddou	✓	✓		✓		✓				✓		✓		

C : **C**onceptualization
M : **M**ethodology
So : **So**ftware
Va : **Va**lidation
Fo : **Fo**rmal Analysis
I : **I**nvestigation
R : **R**esources
D : **D**ata Curation
O : Writing - **O**riginal Draft
E : Writing - Review & **E**diting
Vi : **Vi**sualization
Su : **Su**pervision
P : **P**roject Administration
Fu : **Fu**nding Acquisition

CONFLICT OF INTEREST STATEMENT

Authors state no conflict of interest.

DATA AVAILABILITY

The data and MATLAB simulation code that support the findings of this study are available from the corresponding author upon reasonable request.

REFERENCES

[1] K. Technologies, "6G : Going Beyond 100 Gbps to 1 Tbps," *Ericsson Technology Review*, pp. 1–7, 2021, [Online]. Available: http://www.keysight.com/

[2] R. Hadani and A. Monk, "OTFS: A New Generation of Modulation Addressing the Challenges of 5G," 2018, *arXiv*. doi: 10.48550/ARXIV.1802.02623.

[3] W. Yuan *et al*., "New delay Doppler communication paradigm in 6G era: A survey of orthogonal time frequency space (OTFS)," *China Communications*, vol. 20, no. 6, pp. 1–25, 2023, doi: 10.23919/JCC.fa.2022-0578.202306.

[4] W. Saad, M. Bennis, and M. Chen, "A Vision of 6G Wireless Systems: Applications, Trends, Technologies, and Open Research Problems," *IEEE Network*, vol. 34, no. 3, pp. 134–142, 2020, doi: 10.1109/MNET.001.1900287.

[5] Y. Li and G. L. Stüber, Eds., Orthogonal Frequency Division Multiplexing for Wireless Communications. in Signals and Communication Technology. *Boston: Kluwer Academic Publishers*, 2006. doi: 10.1007/0-387-30235-2.

[6] A. Farhang, A. RezazadehReyhani, L. E. Doyle, and B. Farhang-Boroujeny, "Low Complexity Modem Structure for OFDM-Based Orthogonal Time Frequency Space Modulation," *IEEE Wireless Communications Letters*, vol. 7, no. 3, pp. 344–347, Jun. 2018, doi: 10.1109/LWC.2017.2776942.

[7] T. Zemen and C. F. Mecklenbräuker, "Time-variant channel estimation using discrete prolate spheroidal sequences," *IEEE Transactions on Signal Processing*, vol. 53, no. 9, pp. 3597–3607, 2005, doi: 10.1109/TSP.2005.853104.

[8] M. Aldababsa, S. Ozyurt, G. K. Kurt, and O. Kucur, "A Survey on Orthogonal Time Frequency Space Modulation," *IEEE Open Journal of the Communications Society*, vol. 5, pp. 4483–4518, 2024, doi: 10.1109/OJCOMS.2024.3422801.

[9] R. Hadani *et al*., "Orthogonal Time Frequency Space Modulation," *Orthogonal Time Frequency Space Modulation*, Aug. 2018, *arXiv*. doi: 10.48550/ARXIV.1808.00519.

[10] P. Raviteja, K. T. Phan, Y. Hong, and E. Viterbo, "Interference cancellation and iterative detection for orthogonal time frequency space modulation," *IEEE Transactions on Wireless Communications*, vol. 17, no. 10, pp. 6501–6515, 2018, doi: 10.1109/TWC.2018.2860011.

[11] P. Raviteja, K. T. Phan, Q. Jin, Y. Hong, and E. Viterbo, "Low-complexity iterative detection for orthogonal time frequency space modulation," *IEEE Wireless Communications and Networking Conference, WCNC*, vol. 2018-April, pp. 1–6, 2018, doi: 10.1109/WCNC.2018.8377159.

[12] Z. Wei, S. Li, W. Yuan, R. Schober, and G. Caire, "Orthogonal Time Frequency Space Modulation - Part I: Fundamentals and Challenges Ahead," *IEEE Communications Letters*, vol. 27, no. 1, pp. 4–8, 2023, doi: 10.1109/LCOMM.2022.3209689.

[13] A. Darghouthi, A. Khlifi, H. Shaiek, F. B. Salah, and B. Chibani, "An hybrid framework OTFS-OFDM based on mobile speed estimation," *International Journal of Computer Networks & Communications*, vol. 16, no. 3, pp. 49–67, May 2024, doi: 10.5121/ijcnc.2024.16304.

[14] I. G. Astudillo, "Performance comparison of OTFS vs OFDM wireless signals in high-mobility environments," Bachelor thesis, Universitat Politècnica de Catalunya, Barcelona, Spain, 2026. [Online]. Available: https://upcommons.upc.edu/server/api/core/bitstreams/5f776267-646d-4a0d-9db7-c2656245291d/content.

[15] A. Darghouthi, A. Khlifi, B. Chibani, and H. Shaiek, "OTFS vs OFDM Waveforms Switching Use based on Mobile Speed Estimation," *Wireless Personal Communications*, vol. 139, no. 3, pp. 1499–1513, 2024, doi: 10.1007/s11277-024-11671-6.

[16] M. Schwartz, Mobile Wireless Communications. *Cambridge University Press*, 2004. doi: 10.1017/CBO9780511811333.

[17] T. M. C. Chu and H.-J. Zepernick, "Modulation and Detection for High Doppler Channels: An Overview on OTFS Modulation," *Publication Blekinge Institute of Technology*, 2023.

[18] D. Bandeira, D. Le Ruyet, M. Pischella, and J. Mota, "Performance Evaluation of Low-Complexity Algorithms for Orthogonal

Time-Frequency Space Modulation," *Journal of Communication and Information Systems*, vol. 35, no. 1, pp. 138–149, 2020, doi: 10.14209/jcis.2020.15.
[19] A. Compagnoni, R. Tuninato, C. F. Chiasserini, R. Garello, A. Nordio, and E. Viterbo, "OTFS vs. OFDM in High-speed Vehicular Traffic Scenarios," *IEEE Wireless Communications and Networking Conference*, WCNC, 2025, doi: 10.1109/WCNC61545.2025.10978670.
[20] S. H. Khadum, T. M. Jamel, and H. F. Kkhazaal, "Performance and evaluation of OTFS modulation systems using different high mobility channels," *International Journal of Electronics and Telecommunications*, vol. 71, no. 2, pp. 505–512, Jan. 2025, doi: 10.24425/ijet.2025.153598.
[21] J. M. L. B. Filho, D. Pena, M. C. Muniz, A. A. M. de Medeiros, and V. Sousa, "Comparative Performance Analysis of OTFS and OFDM Modulations for Mobile Wireless Communications," in *Anais do XLIII Simpósio Brasileiro de Telecomunicações e Processamento de Sinais, Sociedade Brasileira de Telecomunicações*, 2025, doi: 10.14209/sbrt.2025.1571156218.
[22] C. Xu *et al*., "OTFS-Aided RIS-Assisted SAGIN Systems Outperform Their OFDM Counterparts in Doubly Selective High-Doppler Scenarios," *IEEE Internet of Things Journal*, vol. 10, no. 1, pp. 682–703, 2023, doi: 10.1109/JIOT.2022.3203895.
[23] A. Shafie, J. Yuan, P. Fitzpatrick, T. Sakurai, and Y. Fang, "On the Coexistence of OTFS Modulation With OFDM-Based Communication Systems," *IEEE Transactions on Communications*, vol. 72, no. 11, pp. 6822–6838, 2024, doi: 10.1109/TCOMM.2024.3412776.
[24] S. Srivastava, R. K. Singh, A. K. Jagannatham, A. Chockalingam, and L. Hanzo, "OTFS Transceiver Design and Sparse Doubly-Selective CSI Estimation in Analog and Hybrid Beamforming Aided mmWave MIMO Systems," *IEEE Transactions on Wireless Communications*, vol. 21, no. 12, pp. 10902–10917, Dec. 2022, doi: 10.1109/TWC.2022.3188040.
[25] T. Thaj and E. Viterbo, "Low Complexity Iterative Rake Decision Feedback Equalizer for Zero-Padded OTFS Systems," *IEEE Transactions on Vehicular Technology*, vol. 69, no. 12, pp. 15606–15622, Dec. 2020, doi: 10.1109/TVT.2020.3044276.

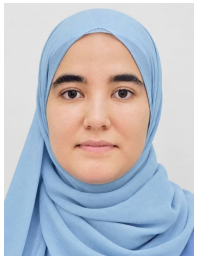
BIOGRAPHIES OF AUTHORS



Nessrine Smaili received the State Engineering degree (Ingéniorat d'État) in Electrical Engineering (Electronics) in 2011 from the ex-INELEC, University of Boumerdes, Algeria, and the Magister degree in Electronics (Telecommunications) in 2014 from the Military Polytechnic School (EMP), Algiers, Algeria, and the Ph.D. degree from ex-INELEC, University of Boumerdes, Algeria. She is currently a senior lecturer and researcher at ex-INELEC, University of Boumerdes. Her research interests are in applied signal processing to digital communication and wireless and mobile communication. She can be contacted at email: n.smaili@univ-boumerdes.dz.



Dihia Amani received the State MASTER's degree in Electrical and Electronics Engineering (Télécommunications) in 2025 from the ex-INELEC, University of Boumerdes, Algeria. She can be contacted at email: amanidihia@gmail.com.



Feriel Razaoui received the State MASTER's degree in Electrical and Electronics Engineering (Télécommunications) in 2025 from the ex-INELEC, University of Boumerdes, Algeria. She can be contacted at email: feryelrazaoui6@gmail.com.



Mustapha Djeddou received the State Engineering degree (Ingéniorat d'État) in Electrical Engineering (Electronics) in 1991 from the Military Polytechnic School (EMP), Algiers, Algeria, and the Magister degree in Electronics (Telecommunications) in 1998 and the Ph.D. degree from ENP in 2005 from the National Polytechnic School (ENP). He is currently a senior lecturer and researcher at ENP. His research interests are in applied signal processing to radar and digital communication, wireless and mobile communication. He can be contacted at email: mustapha.djeddou@g.enp.edu.dz.